LOCALIZATION AND SHEAR BANDS IN HIGH STRAIN-RATE PLASTICITY

THEODOROS KATSAOUNIS* AND ATHANASIOS TZAVARAS†

Abstract. This article is devoted to the explanation of the onset of localization and the formation of shear bands in high strain-rate plasticity of metals. We employ the Arrhenius constitutive model and show Hadamard instability for the linearized problem. For the nonlinear model, using an asymptotic procedure motivated by the theory of relaxation and the Chapman-Enskog expansion, we derive an effective equation for the evolution of the strain rate, which is backward parabolic with a small stabilizing fourth order correction. We construct self-similar solutions that describe the self-organization into a localized solution starting from well prepared data.

Key words. shear bands, localization, effective equations, self-similarity.

AMS(MOS) subject classifications. 74C20, 74H35, 35F55, 35K55, 35Q72.

1. Introduction. The phenomenon of shear strain localization appears in several instances of material instability in mechanics. It is associated with ill-posedness of an underlying initial value problem, what has coined the term Hadamard-instability for its description in the mechanics literature. It should however be noted that while Hadamard instability indicates the catastrophic growth of oscillations around a mean state, it does not by itself explain the formation of coherent structures typically observed in localization. The latter is a nonlinear effect that will be the center-stage of the present study.

The mathematical theory of localization in high strain rate plasticity aims to understand a destabilizing feedback mechanism proposed in [20, 3] and deemed responsible for formation of shear band. It poses analytical challenges at the interface of dynamical systems theory and (small viscosity) parabolic regularizations for ill-posed problems. The onset of localization may be decomposed into two stages. At the first stage (a) one aims to determine whether a Hadamard-type instability is at play for a linearized problem. The second stage (b) requires to understand how the Hadamard instability interacts with the nonlinear features of the problem to form a localized coherent state, associated to a shear band. The latter is a challenging problem in the realm of nonlinear analysis. In this survey we draw material from [10, 11, 1] and focus on the Arrhenius law as a paradigm to describe the sequence of events occurring in the process of localization.

*Department of Applied Mathematics, University of Crete, Heraklion, 71409, Greece and Institute of Applied and Computational Mathematics, FORTH, Heraklion 71110, Greece (thodoros@tem.uoc.gr).

†Department of Applied Mathematics, University of Crete, Heraklion, 71409, Greece; and Institute of Applied and Computational Mathematics, FORTH, Heraklion, 71110, Greece (tzavaras@tem.uoc.gr).

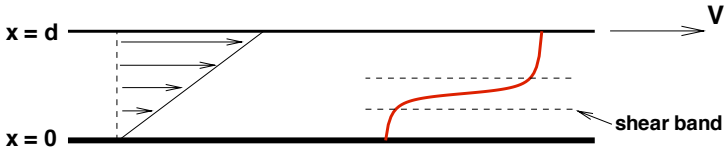

FIG. 1. *Uniform shear versus shear band.*

2. Description of the problem. The formation of shear bands during rapid shearing deformations of steels [4, 9, 20] is a striking instance of material instability in mechanics. The shear strain concentrates in a narrow band inside the specimen and concurrently an elevation of the temperature occurs in the interior of the band. A caricature of shear band forming is presented in Fig. 1. Shear bands are often precursors to rupture and their study has attracted considerable attention in the mechanics and mathematics literature including experimental works [4, 9], mechanical modeling and linearized analysis studies ([3, 8, 12, 17, 19] and references therein), asymptotic analysis [6, 18], nonlinear analysis [5, 13, 14, 2], and numerical investigations [16, 7, 1].

2.1. Modeling shear bands. Shear bands appear and propagate as one dimensional structures (up to interaction times), and most investigations have focused on the study of one-dimensional, simple shearing deformations. As a test problem we consider the simple shear between two parallel plates of a thermoviscoplastic material, Fig. 1. The associated model (see [3, 17, 10] for details) reads

$$\begin{aligned} v_t &= \frac{1}{r}\,\sigma_x, \\ \theta_t &= \kappa\theta_{xx} + \sigma\gamma_t, \\ \gamma_t &= v_x, \end{aligned} \tag{2.1}$$

where r, κ are non-dimensional constants. The variables, velocity in the shearing direction $v(x,t)$, the (plastic) shear strain $\gamma(x,t)$, the temperature $\theta(x,t)$, the heat flux $Q(x,t)$, and the shear stress $\sigma(x,t)$, are connected through the balance of linear momentum, kinematic compatibility, and the balance of energy equations.

It was recognized by Zener and Hollomon [20] that the effect of the deformation speed is twofold: First, an increase in the deformation speed changes the deformation conditions from isothermal to nearly adiabatic. Under such conditions the combined effect of thermal softening and strain hardening tends to produce net softening response. (Indeed, experimental observations of shear bands are typically associated with strain softening response – past a critical strain – of the measured stress-strain curve [3].) Second, strain rate has an effect *per se*, and needs to be included in the constitutive modeling. Accordingly, a model is employed where the shear

stress is described by a constitutive law within the framework of thermoviscoplasticity: $\sigma = f(\theta, \gamma, \gamma_t)$ with $f_p > 0$. This may be viewed as a plastic flow rule or a yield surface, what suggests the terminology: the material exhibits thermal softening at state variables (θ, γ, p) where $f_\theta(\theta, \gamma, p) < 0$, strain hardening at state variables where $f_\gamma(\theta, \gamma, p) > 0$, and strain softening when $f_\gamma(\theta, \gamma, p) < 0$. The slopes of f measure the degree of thermal softening, strain hardening (or softening) and strain-rate sensitivity, respectively. The difficulty of performing high strain-rate experiments causes uncertainty as to the specific form of the constitutive form of the stress. In the literature two constitutive laws are widely used to describe the stress σ: the *power law* and the *Arrhenius law*,

$$\sigma = \theta^{-\alpha}\gamma^m\gamma_t^n, \qquad \text{Power Law}, \tag{2.2}$$

$$\sigma = e^{-\alpha\theta}v_x^n, \qquad \text{Arrhenius Law}. \tag{2.3}$$

The upper plate at $x = 1$ is subjected to a prescribed constant velocity $V = 1$ (in non-dimensional variables) while the lower plate at $x = 0$ is held at rest: $v(0, t) = 0$, $v(1, t) = 1$. It is further assumed that the plates are thermally insulated: $\theta_x(0, t) = 0$, $\theta_x(1, t) = 0$. For the heat flux Q one either uses the adiabatic assumption $Q = 0$ (equivalently $\kappa = 0$) or alternatively a Fourier law $Q = \kappa\theta_x$ with thermal diffusivity parameter κ. Imposing adiabatic conditions projects the belief that, at high strain rates, heat diffusion operates at a slower time scale than the one required for the development of a shear band. It appears a plausible assumption for the shear band initiation process, but not necessarily for the evolution of a developed band, due to the high temperature differences involved.

We summarize the equations describing the model. For the case of the power law the resulting system reads

$$\begin{aligned} v_t &= \frac{1}{r}\,\sigma_x, \\ \theta_t &= \kappa\theta_{xx} + \sigma\gamma_t, \\ \gamma_t &= v_x, \\ \sigma &= \theta^{-\alpha}\gamma^m\gamma_t^n\,. \end{aligned} \tag{2.4}$$

The Arrhenius law does not exhibit any strain hardening and thus the system decouples and leads to the form

$$\begin{aligned} v_t &= \frac{1}{r}\,\sigma_x, \\ \theta_t &= \kappa\theta_{xx} + \sigma v_x \\ \sigma &= e^{-\alpha\theta}v_x^n\,. \end{aligned} \tag{2.5}$$

In the sequel we focus on the Arrhenius model (2.5); we refer to [10, 11] for analogous results for the power law.

The models (2.4) and (2.5) admit a class of special solution describing uniform shearing. For the Arrhenius model (2.5), the uniform shear flow is

$$\begin{aligned} v_s &= x, \\ \theta_s &= \frac{1}{\alpha}\log(\alpha t + k_0), \quad k_0 = e^{\alpha\theta_0}, \\ \sigma_s &= \frac{1}{\alpha t + k_0}. \end{aligned} \tag{2.6}$$

The graph $\sigma - t$ is viewed as describing the stress vs. average strain response. As the graph is always decreasing, it means that there is always net softening response.

2.2. Analytical challenges posed by the localization problem. In this review work we focus on the initiation stage of shear bands and seek to understand the mechanism of formation. There are the following tasks to be carried out :

- To define a notion of stability (or instability) for the uniform shear; this task is complicated by the time dependent nature of the base solutions.
- To derive quantitative criteria for stability (or instability) and a mathematical mechanism pinpointing the onset of localization.
- To describe the localization process and the formation of the shear band.

Naturally, one distinguishes two stages in the process: The initial stage of stability or instability of the uniform shearing solutions leads to questions in the realm of linearized analysis, but with certain special features. Because the uniform shearing solution is time dependent the notion of stability has to be specified. An efficient definition due to Molinari and Clifton [12, 8] espouses the idea of relative perturbation. That is, the uniform shear is stable if perturbations grow slower than the base solutions, and unstable if perturbations grow faster than the base solution. Following that framework leads to questions of linearized stability analysis for non-autonomous linear systems. A rigorous analysis for a simplified model illustrating the difficulties can be found in [15]. In section 3 we carry out this program for the Arrhenius model (2.5).

The second stage of localization lies within the realm of nonlinear analysis, and the focal issue is how the catastrophic growth of high frequency oscillations resulting from Hadamard instability interacts with the nonlinearity to form a coherent structure. A quantitative criterion accounting for the nonlinear aspects of localization was recently derived in [10], based on ideas from the theory of relaxation system and the Chapman Enskog expansion. In follow-up work [11], this analysis is supplemented with a study of self-similar solutions associated with a time-reversed problem with delta-mass initial data. Numerical investigations of the self-similar solutions indicate how the localized state evolves from well prepared initial data for

a power law. The corresponding analysis for the Arrhenius system is presented in sections 5 and 6. We refer to [10] and [11] for analogous results for system (2.4).

3. Stability of the Arrhenius system. We introduce new variables $(V,\ \Theta,\ \Sigma)$ that describe the relative change of a solution to (2.5) with respect to the uniform shear flow (2.6):

$$\begin{aligned} v &= V(x,\tau(t)),\\ \theta &= \theta_s(t) + \Theta(x,\tau(t)),\\ \sigma &= \sigma_s(t)\Sigma(x,\tau(t))\,, \end{aligned} \tag{3.1}$$

where $\tau(t)$ is a rescaling of time, defined by

$$\dot\tau(t) = \sigma_s(t) = \frac{1}{\alpha t + k_0}, \quad \tau(0) = 0, \implies \tau(t) = \frac{1}{\alpha}\log\left(\frac{\alpha}{k_0}t + 1\right).$$

The new variables (u, Θ, Σ), where $u = V_x$ satisfy the system

$$\begin{aligned} u_\tau &= \frac{1}{r}\Sigma_{xx},\\ \Theta_\tau &= k_0\kappa e^{\alpha\tau}\Theta_{xx} + (\Sigma u - 1)\,,\\ \Sigma &= e^{-\alpha\Theta}u^n. \end{aligned} \tag{3.2}$$

The uniform shear flow, via (3.1), is mapped to the point

$$u_0 = 1,\ \Theta_0 = 0,\ \Sigma_0 = 1\,,$$

which is an equilibrium of (3.2). Moreover, let us consider the ode system consisting of the second ($\kappa = 0$) and third equation in (3.2),

$$\begin{aligned} \Theta_\tau &= e^{-\alpha\Theta}u^{n+1} - 1,\\ \Sigma &= e^{-\alpha\Theta}u^n. \end{aligned}$$

This system has an equilibrium manifold parametrized by the moment u,

$$(\Theta,\Sigma) = \left(\frac{n+1}{\alpha}\log u, u^{-1}\right) \quad \text{or} \quad (\Theta,\Sigma) = \left(\Theta, e^{-\frac{\alpha}{n+1}\Theta}\right),$$

and its flow is globally attracted to the equilibrium manifold.

3.1. Linearized stability. We turn to linearized stability for the rescaled system (3.2). We will say that the uniform shear is stable if the perturbation decays and unstable if the perturbation grows. This notion of stability corresponds to the idea of relative perturbation stability analysis in [12] (see also [8, 15]). Consider a perturbation of the uniform shear $\Sigma_0 = 1\,,\ u_0 = 1\,,\ \Theta_0 = 0$, that is

$$
\begin{aligned}
u &= 1 + \delta\, u_1 + O(\delta^2),\\
\Sigma &= 1 + \delta\, \Sigma_1 + O(\delta^2),\\
\Theta &= 0 + \delta\, \Theta_1 + O(\delta^2),
\end{aligned}
$$

and obtain the linearized system

$$
\begin{aligned}
u_{1,\tau} &= \frac{1}{r}\,\Sigma_{1,xx},\\
\Theta_{1,\tau} &= k_0\kappa e^{\alpha\tau}\,\Theta_{1,xx} - \alpha\Theta_1 + (n+1)u_1,\\
\Sigma_1 &= -\alpha\Theta_1 + nu_1,
\end{aligned}
\tag{3.3}
$$

with boundary conditions

$$
\Theta_{1,x}(0,\tau) = \Theta_{1,x}(\pi,\tau) = 0, \quad u_{1,x}(0,\tau) = u_{1,x}(\pi,\tau) = 0.
$$

The solutions of (3.3) can be expressed in terms of the Fourier modes

$$
u_1(x,\tau) = \hat{v}_j(\tau)\cos(jx), \quad \Theta_1(x,\tau) = \hat{\xi}_j(\tau)\cos(jx),
$$

and the Fourier coefficients $(\hat{v}_j, \hat{\xi}_j)$ satisfy the non-autonomous system of ordinary differential equations.

$$
\begin{aligned}
\frac{d\hat{v}_j}{d\tau} &= -j^2\frac{n}{r}\hat{v}_j + j^2\frac{\alpha}{r}\hat{\xi}_j,\\
\frac{d\hat{\xi}_j}{d\tau} &= -j^2 k_0\kappa e^{\alpha\tau}\hat{\xi}_j - \alpha\hat{\xi}_j + (n+1)\hat{v}_j.
\end{aligned}
\tag{3.4}
$$

We proceed to analyze the behavior of solutions to (3.4). When $\kappa = 0$ the system is autonomous and the analysis concludes with an examination of the eigenvalues. When $\kappa \neq 0$ we will consider the problem with the diffusion coefficient frozen in time, and the eigenvalue analysis gives an indication on what to expect (but is not rigorous). Assuming the diffusion coefficient to be frozen in time, consider the ode system:

$$
\frac{d}{dt}\begin{pmatrix}\hat{v}_j\\ \hat{\xi}_j\end{pmatrix} = \begin{pmatrix}-j^2\frac{n}{r} & j^2\frac{\alpha}{r}\\ n+1 & -j^2\kappa-\alpha\end{pmatrix}\begin{pmatrix}\hat{v}_j\\ \hat{\xi}_j\end{pmatrix}.
$$

The characteristic polynomial of the matrix is

$$
\lambda^2 + \lambda\left(j^2\frac{n}{r} + j^2\kappa + \alpha\right) + j^2\left[\frac{n}{r}(j^2\kappa+\alpha) - (n+1)\frac{\alpha}{r}\right] = 0,
$$

and the discriminant

$$
\Delta = j^4(\frac{n}{r}-\kappa)^2 + 2j^2(\frac{n}{r}+\kappa)\alpha + 4j^2\frac{\alpha}{r} + \alpha^2 > 0\,.
$$

The eigenvalues (characteristic speeds) are all real and

$$
\lambda_1\lambda_2 = j^2\left(j^2\kappa\frac{n}{r} - \frac{\alpha}{r}\right) = \frac{j^2}{r}\left(j^2\kappa n - \alpha\right).
$$

Hence, if $j^2\kappa n - \alpha < 0$ then $\lambda_1\lambda_2 < 0$ and there is one positive eigenvalue. In the adiabatic case $\kappa = 0$ we always have

$$\lambda_1 + \lambda_2 < 0 \quad \text{and} \quad \lambda_1\lambda_2 = -j^2\frac{\alpha}{r} < 0.$$

We conclude

- If $\kappa = 0$ then for every Fourier mode j there is one positive and one negative eigenvalue, what indicates Hadamard instability.
- If $\kappa \neq 0$ there is one positive eigenvalue for the j-the mode, $j = 1, 2, ...$ if and only if $j^2 n\kappa - \alpha < 0$. Therefore, the first few Fourier modes may well be unstable but for $\kappa \neq 0$ the high frequency modes will decay.

This analysis is rigorous for $\kappa = 0$ but the analysis of frozen coefficients is only suggestive of the actual behavior in the heat conducting case. An exact analysis of the linearized non-autonomous system is carried out in [11] and shows that for $\kappa \neq 0$ the Fourier modes grow initially but after a transient period the inhomogeneities of the state variables eventually dissipate. This suggests the possibility of metastable response even in the nonlinear regime. Indeed, this has been observed numerically [1] for the case of a power law (2.2).

4. Numerical results for the Arrhenius system. We present numerical results for the Arrhenius system obtained by discretizing (2.5). A small initial temperature perturbation of Gaussian form is introduced at the center of the slab, while the initial velocity profile is retained as the uniform shearing solution (2.6). The boundary conditions are

$$v(0,t) = 0, \quad v(1,t) = 1, \quad \theta_x(0,t) = \theta_x(1,t) = 0.$$

The spatial discretization of (2.5) is based on a finite element method using linear elements, while for the temporal discretization we use the implicit Euler method. Special adaptive techniques in space as well as in time are used in order to fully resolve the band, see [1]. We consider adiabatic deformations ($\kappa = 0$) with $\alpha = 0.25$, $n = 0.1$. The numerical solution of the system, up to time $t \sim 7.47$ is shown in Figures 2 and 3. As seen in Figure 3 stress diffusion collapses across the shear band.

5. Derivation of an effective equation. Next, we derive an effective equation describing the long-time behavior of the system (2.5). Our analysis follows [10] adapted here to the case of the Arrhenius model. When $\kappa = 0$ the system (3.2) takes the form

$$\begin{aligned} u_t &= \frac{1}{r}\Sigma_{xx}, \\ \Theta_t &= \Sigma u - 1, \\ \Sigma &= e^{-\alpha\Theta}u^n. \end{aligned} \tag{5.1}$$

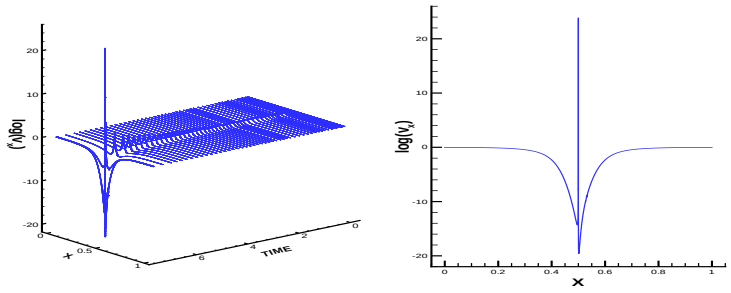

FIG. 2. $v_x(\gamma_t)$ *in log-scale: evolution (left), final time (right).*

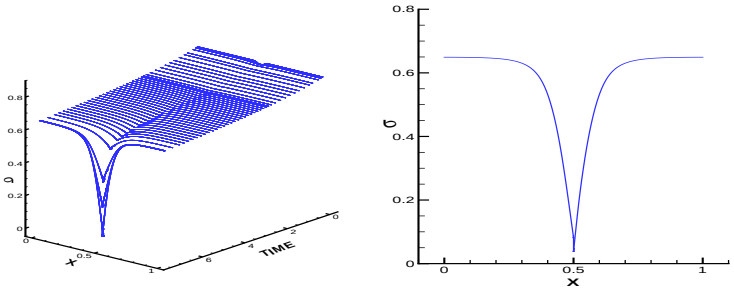

FIG. 3. σ *: evolution (left), final time (right).*

The forthcoming analysis expands on the following view of the problem. We expect that as $t \to \infty$ the first equation in (5.1) will act as a moment equation while the large time behavior of the remaining equations will be slaved into the equilibrium manifold, that is $\Sigma u \to 1$ as $t \to \infty$ and the limiting dynamics is captured by the effective equation

$$u_t = \frac{1}{r}(u^{-1})_{xx}, \tag{5.2}$$

which is a backward parabolic.

To capture this asymptotic behavior of (5.1) we introduce a parameter T thought of as an observational time scale. Consider the time rescaling $s(t) = t/T$, then

$$\begin{aligned} &u_s = \frac{T}{r}\Sigma_{xx}, \\ &\frac{1}{T}\Theta_s = (\Sigma u - 1)\,, \\ &\Sigma = e^{-\alpha\Theta}u^n. \end{aligned} \tag{5.3}$$

Moreover, we either consider an inner expansion of the solution (see [11]) or consider a limit where r is also scaled with T and $r = O(T)$. This corresponds to looking at an asymptotic regime where inertia is dominant. We introduce the Hilbert expansion

$$\begin{aligned} u &= u_0 + \frac{1}{T}u_1 + O(\frac{1}{T^2}), \\ \Sigma &= \Sigma_0 + \frac{1}{T}\Sigma_1 + O(\frac{1}{T^2}), \\ \Theta &= \Theta_0 + \frac{1}{T}\Theta_1 + O(\frac{1}{T^2}), \end{aligned} \tag{5.4}$$

and compute the first few terms of the expansion. The $O(1)$ and $O(\frac{1}{T})$ terms give

$$\begin{aligned} O(1): &\quad \Sigma_0 u_0 = 1, \quad \Sigma_0 = e^{-\alpha\Theta_0}u_0^n \implies \Sigma_0 = \frac{1}{u_0}, \quad \Theta_0 = \frac{n+1}{\alpha}\log u_0, \\ O(\frac{1}{T}): &\quad \Theta_{0,s} = \Sigma_1 u_0 + \Sigma_0 u_1, \quad \Sigma_1 = -\alpha\Sigma_0\Theta_1 + n\frac{\Sigma_0}{u_0}u_1, \\ &\implies \Sigma_1 = -\frac{u_1}{u_0^2} + \frac{1}{u_0}\partial_s\left(\frac{n+1}{\alpha}\log u_0\right). \end{aligned}$$

Moreover, (5.3)(a) implies

$$u_{0,s} + \frac{1}{T}u_{1,s} + O(\frac{1}{T^2}) = \partial_{xx}\left(\Sigma_0 + \frac{1}{T}\Sigma_1 + O(\frac{1}{T^2})\right)$$

which in turn yields

$$u_{0,s} = \partial_{xx}\Sigma_0 = \partial_{xx}(\frac{1}{u_0}).$$

Next, we reconstruct the effective equation up to order $O(\frac{1}{T^2})$ using a procedure analogous to the Chapman-Enskog expansion. From (5.3) we get

$$\begin{aligned} u_s &= \partial_{xx}\left(\frac{1}{u_0} - \frac{1}{T}\frac{u_1}{u_0^2} + \frac{1}{T}\frac{1}{u_0}\partial_s\left(\frac{n+1}{\alpha}\log u_0\right)\right) + O(\frac{1}{T^2}), \\ &= \partial_{xx}\left((u_0 + \frac{1}{T}u_1)^{-1} + O(\frac{1}{T^2})\right) + \frac{1}{T}\partial_{xx}\left(\frac{1}{u_0}\frac{n+1}{\alpha}\frac{1}{u_0}u_{0,s}\right) + O(\frac{1}{T^2}). \end{aligned}$$

Hence, u satisfies within $O(\frac{1}{T^2})$ the effective equation

$$u_s = \partial_{xx}\left(\frac{1}{u}\right) + \frac{1}{T}\frac{n+1}{\alpha}\partial_{xx}\left(\frac{1}{u^2}\partial_{xx}\left(\frac{1}{u}\right)\right). \tag{5.5}$$

The first term in the right hand of (5.5) is backward parabolic. Since the coefficient $\frac{n+1}{\alpha} > 0$, the fourth order term has a regularizing effect.

The uniform shear corresponds to $u_0 = 1$. Set $u = 1 + v$ and compute the linearized equation of (5.5) as follows

$$\begin{aligned}\partial_s v &= \partial_{xx}\left(\frac{1}{1+v} + \frac{1}{T}\frac{n+1}{\alpha}\frac{1}{(1+v)^2}\partial_{xx}\left(\frac{1}{1+v}\right)\right),\\ &= \partial_{xx}\left(1 - v + O(v^2) + \frac{n+1}{T\alpha}(1 - 2v + O(v^2))\partial_{xx}(1 - v + O(v^2))\right),\end{aligned}$$

and thus the linearized equation is

$$\partial_s v = -\partial_{xx} v - \frac{1}{T}\frac{n+1}{\alpha}\partial_{xxxx} v. \tag{5.6}$$

The Fourier transform $\hat{v}$ of v satisfies

$$\partial_s \hat{v} = \left(\xi^2 - \frac{1}{T}\frac{n+1}{\alpha}\xi^4\right)\hat{v},$$

and thus the low frequencies will grow but the high frequency modes still decay since $\frac{n+1}{\alpha} > 0$. Hence the linearized equation (5.6) is well posed.

6. Localization. In this section we show that the effective equation (5.5) admits solutions that develop coherent localized states for well-prepared data. Consider the equation

$$u_t = \partial_{xx}\left(\frac{1}{u}\right) + \varepsilon\partial_{xx}\left(\frac{1}{u^2}\partial_{xx}\left(\frac{1}{u}\right)\right). \tag{6.1}$$

Rescalings of the form

$$u_\lambda = \lambda^\alpha u(\lambda x, \lambda^\beta t) \tag{6.2}$$

leave (6.1) invariant whenever $2\alpha + \beta = 2$. If the scaling is also required to be consistent with conservation of the L^1 mass this fixes the parameters as $\alpha = 1$ and $\beta = 0$.

We seek solutions of (6.1) of the form

$$u = \frac{1}{R(t)}U\left(\frac{x}{R(t)}\right) \tag{6.3}$$

where $R(t)$ decays in time, so that the self-similar solution remains constant on lines $x = \xi R(t)$ focusing to $x = 0$ as $t \to \infty$. Introducing the *ansatz* (6.3) to (6.1), we obtain

$$-\frac{\dot{R}}{R}(\xi U)' = \left(\frac{1}{U} + \varepsilon\frac{1}{U^2}\left(\frac{1}{U}\right)''\right)''.$$

Set $R(t) = e^{-t}$ in which case the form of (6.3) becomes

$$u(x,t) = e^t U\left(x\, e^t\right). \tag{6.4}$$

We look to identify a symmetric profile $U(\xi)$, where $U(0) = U_0 > 0$ and the $U''(0) = -\zeta < 0$ are given as parameters. For an even profile $U'(0) = U'''(0) = 0$. Hence, U is selected by solving the initial value problem

$$\begin{aligned} \xi U &= \left(\frac{1}{U} + \varepsilon \frac{1}{U^2} \left(\frac{1}{U} \right)'' \right)' \\ U(0) = U_0\,, &\quad U'(0) = 0\,, \quad U''(0) = -\zeta\,, \end{aligned} \tag{6.5}$$

where $U_0 > 0$ and $\zeta > 0$ are parameters.

The limiting problem for $\varepsilon = 0$,

$$\begin{aligned} \xi U &= \left(\frac{1}{U} \right)' \\ U(0) &= U_0 > 0\,, \end{aligned} \tag{6.6}$$

can be solved explicitly and its solution reads

$$U(\xi) = \frac{U_0}{(\xi^2 U_0^2 + 1)^{\frac{1}{2}}}\ . \tag{6.7}$$

In turn, it induces the following form for the associated solution u of (6.1) with $\varepsilon = 0$

$$u(x,t) = e^t U(x\, e^t) = \frac{U_0}{(U_0^2 x^2 + e^{-2t})^{\frac{1}{2}}}\ . \tag{6.8}$$

Observe that $u(0,t) = e^t$ grows exponentially at the origin $x = 0$, also that away from $|x| << 1$ the solution $u(x,t) \sim \frac{1}{|x|}$ for any $t > 1$. The solution is formally consistent with conservation of mass and is constant on lines $x = \xi e^{-t}$. This behavior indicates localization.

The problem (6.5) is solved numerically. We ask U to be an even function with normalized value $U(0) = 1$ and with $U''(0) = -\zeta$. We solve for various values of the parameter $\zeta > 0$. The solution of the o.d.e in the limiting $\varepsilon = 0$ case is $U_\infty(\xi) = 1/\sqrt{\xi^2 + 1}$. In Figure 4 the profiles of solutions U are presented for a fixed value of $\zeta = 10$ and three values of ϵ. The profile of U_∞ numerically coincides with the one of value $\epsilon = 0.001$. From the numerical results some observations can be made :

- The profile of U for large values of ξ behaves like $U(\xi) \sim 1/\xi$, independently of ϵ and ζ.
- Oscillations appear in the computed profile in accordance with expectations. The appearance and the frequency of oscillations is strongly related to the values of ε and ζ, but no definitive conclusion can be drawn from the numerical results.

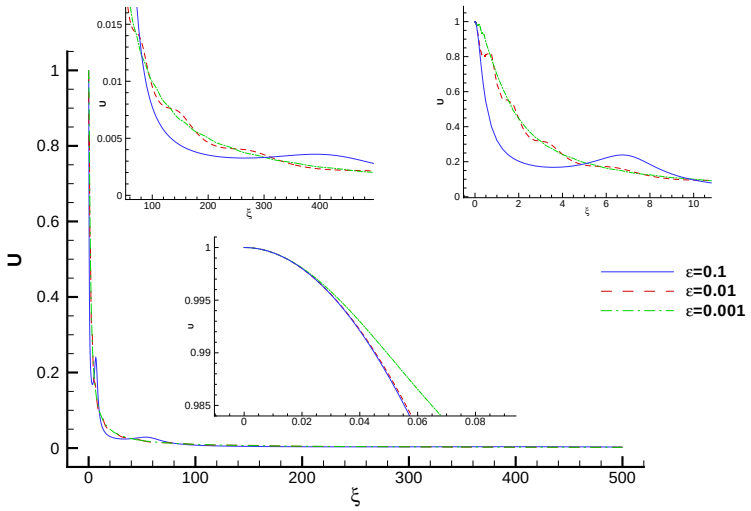

FIG. 4. $\zeta = 10,\ \epsilon \in [5 \cdot 10^{-4}, 5 \cdot 10^{-2}]$.

Acknowledgments. We thank Professor LEV TRUSKINOVSKY for very insightful remarks. AET partially supported by the National Science Foundation. Research partially supported by the European Union FP7 program Capacities (Regpot 2009-1).

REFERENCES

[1] TH. BAXEVANIS, TH. KATSAOUNIS, AND A.E. TZAVARAS, *Adaptive finite element computations of shear band formation*, Math. Models Meth. Appl. Sciences (2010), in press.

[2] M. BERTSCH, L.A. PELETIER, AND S.M. VERDUYN LUNEL, *The effect of temperature dependent viscosity on shear flow of incompressible fluids*, SIAM J. Math. Anal., **22** (1991), 328–343.

[3] R.J. CLIFTON, J. DUFFY, K.A. HARTLEY, AND T.G. SHAWKI, *On critical conditions for shear band formation at high strain rates*, Scripta Met., **18** (1984), pp. 443–448.

[4] L.S. COSTIN, E.E. CRISMAN, R.H. HAWLEY, AND J. DUFFY, *On the localization of plastic flow in mild steel tubes under dynamic torsional loading*, In "Proc. 2nd Conf. on the Mechanical Properties of Materials at high rates of strain", Inst. Phys. Conf. Ser. no 47, Oxford, **90**, 1979.

[5] C.M. DAFERMOS AND L. HSIAO, *Adiabatic shearing of incompressible fluids with temperature dependent viscosity*, Quart. Appl. Math., **41** (1983), 45–58.

[6] J.A. DILELLIO AND W.E. OLMSTEAD, *Shear band formation due to a thermal flux inhomogeneity*, SIAM J. Appl. Math., **57** (1997), 959–971.

[7] D.J. ESTEP, S.M.V. LUNEL, AND R.D. WILLIAMS, *Analysis of shear layers in a fluid with temperature-dependent viscosity*, Comp. Physics, **173** (2001), 17–60.

[8] C. FRESSENGEAS AND A. MOLINARI, *Instability and localization of plastic flow in shear at high strain rates*, J. Mech. Phys. Solids **35** (1987), pp. 185–211.

[9] K.A. Hartley, J. Duffy, and R.J. Hawley, *Measurement of the temperature profile during shear band formation in steels deforming at high-strain rates*, J. Mech. Physics Solids, **35** (1987), 283–301.

[10] Th. Katsaounis and A.E. Tzavaras, *Effective equations for localization and shear band formation*, SIAM J. of Applied Math., **69**, no. 6 (2009), pp. 1618–1643.

[11] Th. Katsaounis and A.E. Tzavaras, *Self-similar organization of localization in high strain-rate plasticity*, in preparation.

[12] A. Molinari and R.J. Clifton, *Analytical characterization of shear localization in thermoviscoplastic materials*, J. Appl. Mech., **54** (1987), 806–812.

[13] A.E. Tzavaras, *Effect of thermal softening in shearing of strain-rate dependent materials*, Arch. Rational Mech. Analysis, **99** (1987), 349–374.

[14] A.E. Tzavaras, *Strain softening in viscoelasticity of the rate type*, J. Integral Equations Appl., **3** (1991), 195–238.

[15] A.E. Tzavaras, *Nonlinear analysis techniques for shear band formation at high strain rates*, Appl. Mech. Reviews, **45** (1992), S82–S94.

[16] J.W. Walter, *Numerical experiments on adiabatic shear band in one space dimension*, Int. J. of Plasticity, **8** (1992), 657–693.

[17] T.W. Wright and J.W. Walter, *On stress collapse in adiabatic shear bands*, J. Mech. Phys. Solids, **35** (1988), 701–720.

[18] T.W.Wright and H. Ockendon, *A model for fully formed shear bands*, J. Mech. Phys. Solids, **40** (1992), 1217–1226.

[19] T.W. Wright, *The Physics and Mathematics of Shear Bands*, Cambridge University Press, 2002.

[20] C. Zener and J.H. Hollomon, *Effect of strain rate upon plastic flow of steel*, J. Appl. Physics, **15** (1944), 22–32.